

# Parton Content of Real and Virtual Photons

I. Schienbein<sup>a</sup>

<sup>a</sup>Institut für Physik, Universität Dortmund  
D-44221 Dortmund, Germany (e-mail: schien@hal1.physik.uni-dortmund.de)

Parameter-free and perturbatively stable leading order (LO) and next-to-leading order (NLO) parton densities for real and virtual photons are presented.

## 1. Introduction

The partonic content of real and virtual photons can be measured, for example, in electron positron scattering. The measured  $e^+e^-$  cross section can be obtained by a convolution of a flux of target photons [1] with the cross section of deep inelastic electron photon scattering

$$d\sigma(ee \rightarrow eX) = f_{\gamma(P^2)/e} * d\sigma(e\gamma(P^2) \rightarrow eX) + \mathcal{O}(P^2/Q^2). \quad (1)$$

The virtuality of the target photon,  $P^2$ , has to be much smaller than the virtuality  $Q^2$  of the probe photon such that the neglected terms of order  $\mathcal{O}(P^2/Q^2)$  are small.

In the following, we are interested in the photon structure function  $F_2^{\gamma(P^2)}(x, Q^2)$  which enters the deep inelastic electron photon cross section in exactly the same way as is well known from deep inelastic electron proton scattering

$$\frac{d\sigma(e\gamma(P^2) \rightarrow eX)}{dx dQ^2} \propto (1 + (1-y)^2) F_2^{\gamma(P^2)} - y^2 F_L^{\gamma(P^2)}. \quad (2)$$

$F_2^{\gamma(P^2)}$  is a convolution of the *massless* parton densities of the real or virtual photon with the respective *massless* Wilson coefficients, in order to obtain a factorization scheme independent, i. e., physically meaningful result [2]

$$F_2^{\gamma(P^2)}(x, Q^2) = \sum_{u,d,s} 2xe_q^2 \times \left[ q^{\gamma(P^2)} + \frac{\alpha_s}{2\pi} (C_q * q^{\gamma(P^2)} + C_g * g^{\gamma(P^2)}) \right]$$

$$+ \frac{\alpha}{2\pi} e_q^2 C_\gamma \Big]. \quad (3)$$

This also holds for the direct photon coefficient  $C_\gamma$ , i. e.,  $C_\gamma$  has to be the massless direct photon coefficient (irrespective of  $P^2$ ) since it is related to the massless photon to quark and photon to gluon splitting functions  $P_{q\gamma}^{(0)}$  and  $P_{g\gamma}^{(0)}$  in the evolution equations.

As usual, we work in NLO in the  $\text{DIS}_\gamma$  scheme in which the destabilizing  $\log(1-x)$  of  $C_\gamma$ , as calculated in the  $\overline{\text{MS}}$  scheme in (3), is absorbed into the quark distributions

$$(q + \bar{q})_{\text{DIS}_\gamma}^\gamma = (q + \bar{q})_{\overline{\text{MS}}}^\gamma + \frac{\alpha}{\pi} e_q^2 C_\gamma^{\overline{\text{MS}}}(x) \\ g_{\text{DIS}_\gamma}^\gamma = g_{\overline{\text{MS}}}^\gamma. \quad (4)$$

Again, it should be emphasized that we use the *real photon* coefficient irrespective of  $P^2$ .

## 2. Boundary Conditions

The parton distributions are then obtained by QCD evolution of appropriate boundary conditions at a low scale  $Q_0^2 \approx 0.3 \text{ GeV}^2$ , which will be presented in the following. The exact LO and NLO values of the universal (i. e. hadron-independent) input scale  $Q_0$  are fixed by the experimentally well constrained radiative parton densities of the proton [3].

### 2.1. Real Photon

The boundary condition for the real photon [2] is given by a vector meson dominance (VMD) ansatz where (at the low scale  $Q_0$ ) the physical photon is assumed to be a coherent superposition

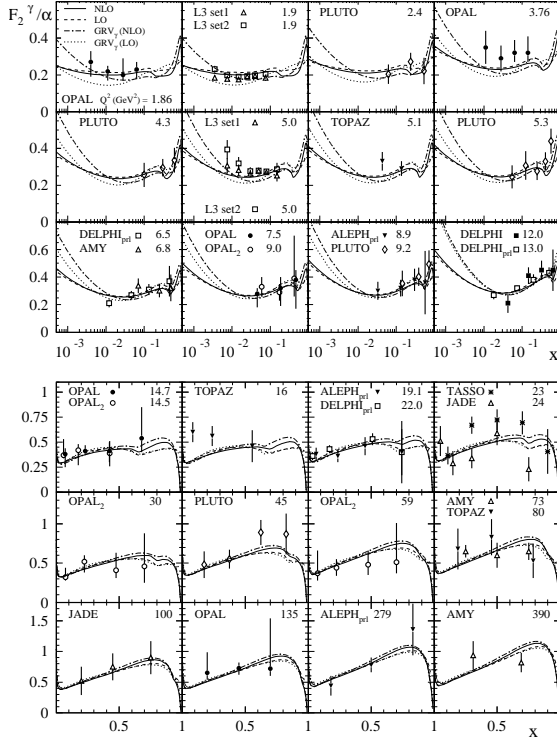


Figure 1. Comparison of our radiatively generated LO and NLO( $\text{DIS}_\gamma$ ) predictions for  $F_2^\gamma(x, Q^2)$ , based on the valence-like parameter-free VMD input in eq. (5), with the data of ref. [7]. For comparison the  $\text{GRV}_\gamma$  [8] results are shown as well. In both cases, the charm contribution has been added, in the relevant kinematic region  $W \geq 2m_c$ , according to fixed order perturbation theory.

of vector mesons which have the same quantum numbers as the photon

$$f^\gamma(x, Q_0^2) = f_{\text{had}}^\gamma(x, Q_0^2) = \alpha G_f^2 f^{\pi^0}(x, Q_0^2) \quad (5)$$

with  $G_{u,d}^2 = (g_\rho \pm g_\omega)^2$  and  $G_g^2 = G_s^2 = g_\rho^2 + g_\omega^2$  ( $g_\rho^2 = 0.50$ ,  $g_\omega^2 = 0.043$ ). This optimal coherence maximally enhances the up quark which is favoured by the experimental data.

Since parton distributions of vector mesons ( $\rho, \omega, \dots$ ) are unknown we furthermore assume that these are similar to pionic parton distributions. Thus, for given pionic parton distributions our model has no free parameter.

## 2.2. Pion

Since only the pionic valence density is experimentally rather well known, we utilize a constituent quark model to relate the pionic light sea and gluon to the much better known parton distributions of the proton [3]. In this model the proton and pion are described by scale independent constituent distributions ( $U^p, U^\pi, \dots$ ) convoluted with their universal partonic content  $f_c$  [4]

$$f^p = \int_x^1 \frac{dy}{y} [U^p(y) + D^p(y)] f_c\left(\frac{x}{y}, Q^2\right) \quad (6)$$

$$f^\pi = \int_x^1 \frac{dy}{y} [U^{\pi^+}(y) + \bar{D}^{\pi^+}(y)] f_c\left(\frac{x}{y}, Q^2\right)$$

where  $f = v, \bar{q}, g$ .

Since in Mellin- $n$ -space the convolution is a simple product, the ratio  $f^\pi/f^p$  is independent of the flavour  $f$  and one can easily find boundary conditions for the pionic gluon and sea which only depend on the rather well determined valence distribution of the pion and the parton distributions of the proton [5,6]

$$g^\pi(n, Q_0^2) = \frac{v^\pi}{v^p} g^p, \quad \bar{q}^\pi(n, Q_0^2) = \frac{v^\pi}{v^p} \bar{q}^p. \quad (7)$$

## 2.3. Virtual Photon

In this subsection boundary conditions for the much more speculative virtual photon are proposed.

First recall that the photonic parton distributions can be written as a sum of a pointlike and a hadronic part

$$f^{\gamma(P^2)}(x, Q^2) = f_{\text{pl}}^{\gamma(P^2)}(x, Q^2) + f_{\text{had}}^{\gamma(P^2)}(x, Q^2). \quad (8)$$

The pointlike part is a particular solution of the inhomogenous evolution equations of the photon and vanishes by definition at the input scale  $\tilde{P}^2 \equiv \max(P^2, Q_0^2)$ :  $f_{\text{pl}}^{\gamma(P^2)}(x, \tilde{P}^2) = 0$ . While the pointlike solution is perturbatively calculable, the homogenous (hadronic) solution requires a boundary condition. At  $\tilde{P}^2$  we assume the hadronic part of the virtual photon to be given by the hadronic part of the real photon suppressed by a rho-meson propagator  $\eta(P^2) = (1 + P^2/m_\rho^2)^{-2}$ :

$$f_{\text{had}}^{\gamma(P^2)}(x, \tilde{P}^2) = \eta(P^2) f_{\text{had}}^\gamma(x, \tilde{P}^2) \quad (9)$$

This boundary condition of course smoothly extrapolates to the real photon case.

Note that, the employed dipole suppression factor is somewhat speculative and can be regarded as the simplest choice of modelling the  $P^2$ -suppression.

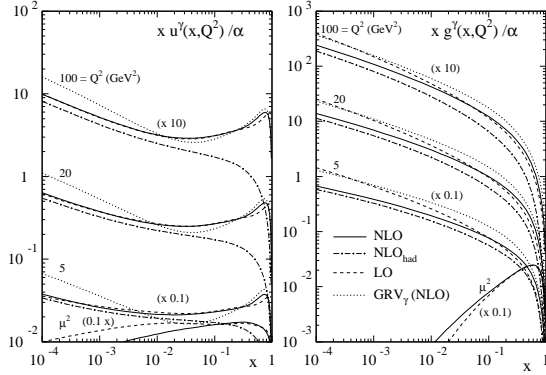


Figure 2. Detailed small- $x$  (as well as large- $x$ ) behavior and predictions of our radiatively generated  $u^\gamma = \bar{u}^\gamma$  and  $g^\gamma$  distributions in LO and NLO(DIS $_\gamma$ ) at fixed values of  $Q^2$ . The dashed-dotted curves show the hadronic NLO contribution  $f_{\text{had}}^\gamma$  to  $f^\gamma$ . The valence-like inputs at  $Q^2 = Q_0^2 \equiv \mu_{\text{LO,NLO}}^2$  [3], according to eq. (5), are shown by the lowest curves referring to  $\mu^2$ . For comparison we show the steeper NLO GRV $_\gamma$  [8] expectations as well. The results have been multiplied by the number indicated in brackets.

### 3. Numerical Results

#### 3.1. Real Photon

In Fig. 1 we compare our LO and NLO predictions for  $F_2^\gamma$ , given by the full and dashed lines, with experimental data [7]. Also shown are the GRV $_\gamma$  [8] predictions which are steeper in the small- $x$  region (due to the steeper sea, which has been generated from a vanishing input). In all cases the charm contribution has been added according to a fixed order calculation (see, e.g., eqs. (15) and (16) in [2]).

As one can see, we achieve a good description of the data, particularly in the region of small  $Q^2$  where the GRV $_\gamma$  and also the SaS 1D [9] expectations fall somewhat below the data. Further-

more, our LO and NLO results are close together demonstrating an excellent perturbative stability.

Figure 2 shows the  $x$ -dependence of the up quark and the gluon for three values of  $Q^2$ . The solid and dashed lines are our NLO and LO results, respectively. The dotted lines are the NLO GRV $_\gamma$  distributions.

Comparing the solid lines with the dashed-dotted lines, representing the hadronic contribution to the solid lines, one can see that for  $x \gtrsim 0.1$  the pointlike part dominates (especially for the quark distribution), whereas at very small  $x$  the hadronic component is dominant implying a small- $x$  behaviour similar to the pion or proton.

Also shown are our valence-like inputs which are (vanishingly) small for  $x \lesssim 10^{-2}$ . Thus, the small- $x$  increase at higher scales is purely due to the QCD evolution.

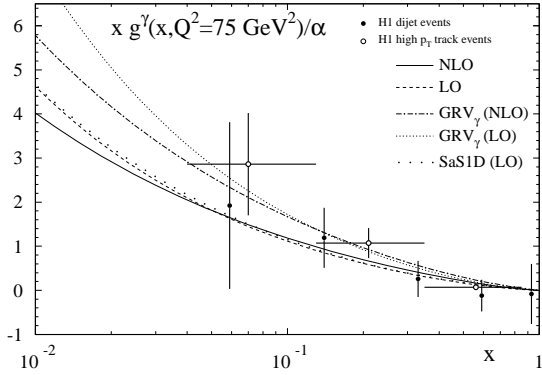


Figure 3. Comparison of our LO and NLO predictions for  $xg^\gamma$  at  $Q^2 \equiv \langle (p_T^{\text{jet}})^2 \rangle = 75 \text{ GeV}^2$  with HERA(H1) measurements [10]. The GRV $_\gamma$  and SaS expectations are taken from refs. [8] and [9], respectively.

In Fig. 3 we compare the  $x$ -dependence of our gluon distribution with recent H1 measurements [10]. The full data points are dijet events and the open points are high  $p_T$  track events. Our LO and NLO results are very similar to the gluon of SaS 1D, shown by the dotted line. The flatter small- $x$  behaviour compared to GRV $_\gamma$  is partly induced by the flatter gluon distribution in the GRV-98 proton [3]. (Another reason is that the

GRV $_{\gamma}$  gluon is enhanced by a factor  $\kappa = 1.6(2.0)$  in NLO (LO) at  $Q_0^2$  in eq. (2) in [8].)

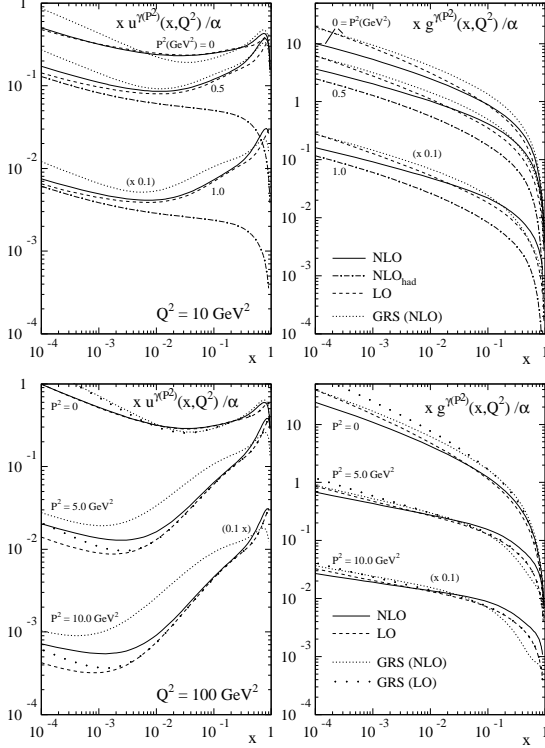


Figure 4. LO and NLO (DIS $_{\gamma}$ ) predictions for the up-quark and gluon distributions of a virtual photon  $\gamma(P^2)$  at  $Q^2 = 10$  and  $100 \text{ GeV}^2$ . For comparison the results for the real photon ( $P^2 = 0$ ) are shown as well. For  $P^2 = 0.5$  and  $1.0 \text{ GeV}^2$  the NLO ‘hadronic’ contribution in (8) is also shown separately. The GRS expectations are taken from ref. [11]. The results have been multiplied by the numbers indicated in brackets.

### 3.2. Virtual Photon

Figure 4 is the virtual photon analogue of Fig. 2. Again the  $x$ -dependence of the up quark and the gluon is shown for two values of  $Q^2$  and several photon virtualities  $P^2$ . The solid and dashed curves are our NLO and LO distributions, respectively, whereas the dotted curves are the NLO predictions of Glück, Reya and Stratmann [11], denoted by GRS. For  $Q^2 = 100 \text{ GeV}^2$  we also

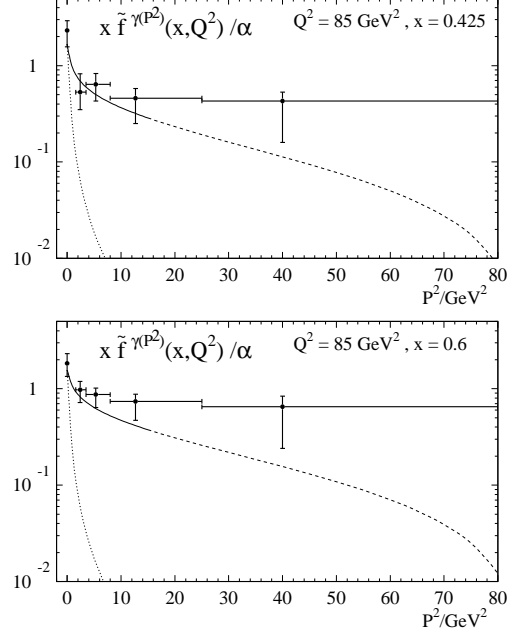


Figure 5. Predictions for the LO effective parton density  $x \tilde{f}^{\gamma(P^2)}(x, Q^2)$  at the scale  $Q^2 \equiv (p_T^{\text{jet}})^2 = 85 \text{ GeV}^2$  and at two fixed values of  $x$ . The H1 data [12] have been extracted from DIS ep dijet production. The solid curves refer to our predictions in the theoretically legitimate region  $P^2 \ll Q^2 \equiv (p_T^{\text{jet}})^2$ , whereas the dashed curves extend into the kinematic region of larger  $P^2$  approaching  $Q^2$  where the concept of parton distributions of virtual photons is not valid anymore (see text).

show the LO GRS up quark distributions (wide dotted), which are very similar to our LO results.

One can see that the pointlike part becomes increasingly important with increasing  $P^2$  due to the dipole suppression of the hadronic component [ $\eta(P^2(\text{GeV}^2) = 0.5, 1.0, 5.0, 10.0) = 0.3, 0.14, 0.01, 0.003$ ]. At  $P^2 = 5, 10 \text{ GeV}^2$  the hadronic part is nearly vanishing even at small  $x$ . Furthermore, note the perturbative stability of the parton distributions guaranteeing the required stability of the physical structure functions.

Finally, in Fig. 5 we compare our LO parton

distributions with an effective parton density

$$\begin{aligned} \tilde{f}^{\gamma(P^2)}(x, Q^2) &= \sum_{q=u,d,s} \left( q^{\gamma(P^2)} + \bar{q}^{\gamma(P^2)} \right) \\ &+ \frac{9}{4} g^{\gamma(P^2)} \end{aligned} \quad (10)$$

which has been extracted from H1 dijet data [12].  $Q \equiv p_T^{\text{jet}}$  and we show results for two values of  $x$  in dependence of the photon virtuality. The transition from the solid to the dashed line indicates that for  $P^2$  approaching  $Q^2$  the concept of renormalization group resummed parton distributions of virtual photons is not expected to hold any more, because the resummed logarithms  $\log Q^2/P^2$  arising in the partonic subprocesses are not much larger than the non-logarithmic terms.

In the relevant kinematic region  $P^2 \ll Q^2$  the agreement with the data is reasonably good. This is in contrast to a simple dipole suppression of the real photon  $\eta(P^2) \tilde{f}^{\gamma(P^2=0)}(x, Q^2)$ , as illustrated by the dotted curves in Fig. 5, which fails to describe the data.

Supported in part by the *Graduiertenkolleg 'Erzeugung und Zerfälle von Elementarteilchen'* of the *Deutsche Forschungsgemeinschaft* at the *Universität Dortmund* and by the *Bundesministerium für Bildung, Wissenschaft, Forschung und Technologie*, Bonn.

## REFERENCES

- V.M. Budnev, I.F. Ginzburg, G.V. Meledin, and V.G. Serbo, *Phys. Rep.* **15**, 181 (1975); S. Frixione, M.L. Mangano, P. Nason, and G. Ridolfi, *Phys. Lett.* **B319**, 339 (1993).
- M. Glück, E. Reya, and I. Schienbein, hep-ph/9903337 (*Phys. Rev. D* (to appear)).
- M. Glück, E. Reya, and A. Vogt, *Eur. Phys. J.* **C5**, 461 (1998).
- G. Altarelli, N. Cabibbo, L. Maiani, and R. Petronzio, *Nucl. Phys.* **B69** (1974) 531.
- M. Glück, E. Reya, M. Stratmann, *Eur. Phys. J.* **C2** (1998) 159.
- M. Glück, E. Reya, I. Schienbein, hep-ph/9903288 (*Eur. Phys. J. C* (to appear)).
- Ch. Berger et al., PLUTO Collab., *Phys. Lett.* **142B**, 111 (1984); *Nucl. Phys.* **B281**, 365 (1987); W. Bartel et al., JADE Collab., *Z. Phys.* **C24**, 231 (1984); M. Althoff et al., TASSO Collab., *Z. Phys.* **C31**, 527 (1986); S.K. Sahu et al., AMY Collab., *Phys. Lett.* **B346**, 208 (1995); T. Kojima et al., AMY Collab., *Phys. Lett.* **B400**, 395 (1997); K. Muramatsu et al., TOPAZ Collab., *Phys. Lett.* **B332**, 477 (1994); K. Ackerstaff et al., OPAL Collab., *Z. Phys.* **C74**, 33 (1997); *Phys. Lett.* **B411**, 387 (1997); *ibid.* **B412**, 225 (1997); P. Abreu et al., DELPHI Collab., *Z. Phys.* **C69**, 223 (1996); F. Kapusta et al., DELPHI Collab., HEP '97 Conference, Jerusalem, August 1997, contribution 416; A. Finch et al., ALEPH Collab., *ibid.*, contribution 607; Photon '97 Conference, Egmond aan Zee, May 1997; ICHEP '98 Conference, Vancouver, July 1998, Abstract No. 898; M. Acciarri et al., L3 Collab., *Phys. Lett.* **B436**, 403 (1998).
- M. Glück, E. Reya, and A. Vogt, *Phys. Rev.* **D45**, 3986 (1992); *ibid.* **D46**, 1973 (1992).
- G.A. Schuler and T. Sjöstrand, *Z. Phys.* **C68**, 607 (1995); *Phys. Lett.* **B376**, 193 (1996).
- T. Ahmed et al., H1 Collab., *Nucl. Phys.* **B445**, 195 (1995); C. Adloff et al., H1 Collab., DESY 98-148 (hep-ex/9810020), *Eur. Phys. J.*, to appear.
- M. Glück, E. Reya, and M. Stratmann, *Phys. Rev.* **D51**, 3220 (1995).
- M.L. Utley, ZEUS Collab., Proceedings of the Int. Europhysics Conf. on HEP '95, Brussels, 1995, eds. J. Lemonne et al., World Scientific, p. 570 (hep-ex/9508016); C. Adloff et al., H1 Collab., *Phys. Lett.* **B415**, 418 (1997); DESY 98-076 (hep-ex/9806029); Paper 544, submitted to the 29th Int. Conf. on HEP ICHEP98, Vancouver, July 1998; DESY-98-205 (hep-ex/9812024).